Estimating Online Influence Needs Causal Modeling! Counterfactual Analysis of Social Media Engagement

Lin Tian & Marian-Andrei Rizoiu
University of Technology Sydney
{Lin.Tian-3,Marian-Andrei.Rizoiu}@uts.edu.au

Abstract

Understanding true influence in social media requires distinguishing correlation from causation—particularly when analyzing misinformation spread. While existing approaches focus on exposure metrics and network structures, they often fail to capture the causal mechanisms by which external temporal signals trigger engagement. We introduce a novel joint treatmentoutcome framework that leverages existing sequential models to simultaneously adapt to both policy timing and engagement effects. Our approach adapts causal inference techniques from healthcare to estimate Average Treatment Effects (ATE) within the sequential nature of social media interactions, tackling challenges from external confounding signals. Through our experiments on real-world misinformation and disinformation datasets, we show that our models outperform existing benchmarks by 15-22% in predicting engagement across diverse counterfactual scenarios, including exposure adjustment, timing shifts, and varied intervention durations. Case studies on 492 social media users show our causal effect measure aligns strongly with the gold standard in influence estimation, the expert-based empirical influence.

1 Introduction

In March 2020, as COVID-19 began its global spread, a simple graphic titled "Flatten the Curve" created by Associate Professor Siouxsie Wiles and cartoonist Toby Morris ignited an unprecedented cascade of social media engagement¹. Within just 72 hours, the visualization accumulated over 10 million impressions on X (formerly Twitter), was translated into more than 25 languages, and was adopted by government health agencies worldwide (Bavel et al., 2020). What made this particular content achieve such extraordinary reach was not merely its clear visualization of pandemic dynamics—it was the complex interplay between its timely release amid escalating global concern, amplification by influential public health accounts, and concurrent spikes in search traffic as reflected in Google Trends data (Jackson et al., 2020). As the graphic's engagement metrics surged, a corresponding peak in "social distancing" searches appeared across global search indices, preceding measurable changes in mobility patterns across affected regions (Gao et al., 2020). Today, with hindsight, we say that the "Flatten the Curve" graphic was influential as it increased the public's awareness of non-pharmaceutical interventions for the COVID-19 pandemic.

But what is influence? It is more than exposure or virality; it is one's capacity to shape attitudes and change behaviors. And while exposure (particularly repeated exposure) and influence are intimately linked, true influence estimation require causal reasoning. This causal perspective on influence has been established in seminal works across multiple disciplines (Aral et al., 2009; Eckles et al., 2016; Watts et al., 2021), which collectively demonstrate that traditional influence measures often conflate homophily with causal effects. In online social media, information cascades equate to exposure—they are the digital equivalent of the *word-of-mouth* phenomenon that allow content to spread widely. But how do they relate to influence? This paper introduces a causal framework to estimate user influence by

¹https://www.washingtonpost.com/graphics/2020/world/corona-simulator/

conducting counterfactual analysis on misinformation and disinformation cascades. This would allow us to understand which users, public groups or pages are truly shaping public discourse on highly polarizing topics, and who does truly drive misinformation spread.

True influence is unobserved, and notoriously difficult to estimate (Ram & Rizoiu, 2024). We therefore train and test our models on observed exogenous attention signals—like search trends, news coverage cycles, or influencer amplification—and ask how do they causally impact content engagement and information diffusion. While existing engagement prediction approaches have made significant progress using content features and network structure (Zhou et al., 2021a), they typically overlook the causal relationship between external temporal signals and engagement dynamics. Moreover, previous studies on influence measurement in social media have often focused on exposure rates and network structures but have not fully incorporated a causal perspective (Cha et al., 2010; Bakshy et al., 2011; Kwak et al., 2010). Similarly, causal inference frameworks in machine learning (Pearl, 2009; Peters et al., 2017) generally lack the temporal sophistication needed to model the intricate dependencies between time-varying external signals and sequential engagement outcomes.

To tackle these challenges, we introduce a causal framework that jointly models treatment intensities – external signals driving engagement – and social engagement outcomes. Our approach builds on advances in sequential modeling, adapting transformer architectures (Vaswani et al., 2017) and selective state space models (e.g., Mamba (Gu & Dao, 2024)) to meet the demands of causal inference with time-varying treatments. By comparing integration mechanisms – token-based, attention-based, layer-based, and adapter-based – we present detailed insights into the architectural requirements for effective causal modeling in social media contexts, particularly in scenarios involving misinformation.

This work explores three key research questions: (1) Does joint modeling of treatment intensities and outcomes improve predictive accuracy under realistic policy-driven scenarios, especially those aimed at curbing misinformation? (2) How effectively do transformers and state space models capture the intricate temporal dependencies between external signals and engagement outcomes? (3) How reliably can these models predict engagement outcomes under hypothetical scenarios, such as changes in exposure rates or policy active timings?

2 Problem Statement

Let $\mathcal E$ denote a social media event with associated posts $\mathcal P=\{p_1,p_2,\ldots,p_N\}$. For each post $p\in\mathcal P$, we define a tuple (t_0,x,u,o,H) where t_0 is the original posting time, x represents the textual content, u captures user metadata, $o\in\mathcal O$ indicates the content category from the set of possible categories $\mathcal O$, and $H=\{(t_j,e_j)\}_{j=1}^m$ is the interval-censored engagement history with m observation intervals. Each e_j is a d-dimensional vector capturing different types of engagement (likes, shares, comments, etc.) at observation time t_j .

The Google Trends information is a set of tuples $G = \{(t_k, g_k)\}_{k=1}^l$, with g_k as a scalar representing the search intensity of keywords related to the post's content (e.g., a spike in searches for "election" for a political post) at time t_k . These signals, collected over l time points, serve as an exogenous signal, capturing how real-world interest.

Given an observation window $\tau_{\rm obs}$ starting at t_0 , let $H_{\tau_{\rm obs}}(p) = \{(t,e) \in H \mid t_0 \leq t \leq t_0 + \tau_{\rm obs}\}$ represent the post's initial engagement history, and $G_{\tau_{\rm obs}} = \{(t,g) \in G \mid t_0 \leq t \leq t_0 + \tau_{\rm obs}\}$ as the corresponding external signals. The goal is to predict the future engagement trajectory under policy-driven modifications to the external signal patterns (e.g., adjusting Google Trends intensity to reflect shifts in public attention). Specifically, we aim to forecast $\{\hat{e}(t_0 + \tau_{\rm obs} + k\Delta t)\}_{k=1}^K$, where Δt is a fixed time step (e.g., one day), and $K = \lfloor T/\Delta t \rfloor$ is the number of prediction points over a horizon T (e.g., one month).

3 Methodology

Our framework (as shown in Fig. 1) models external signals as continuous-intensity treatments through modeling that capture both immediate responses and long-range dependen-

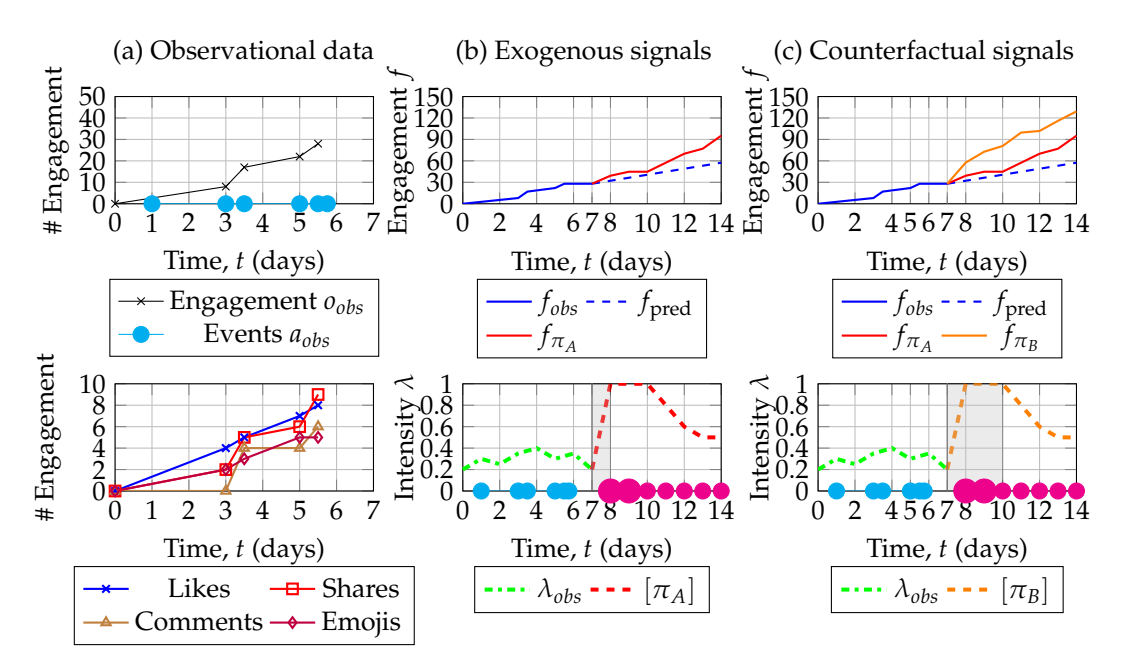


Figure 1: Visualization of engagement data and queries for social media post p. (a) Observational data during the period [0,7] days. The top plot shows cumulative engagement over time (black line with crosses) and observed events (cyan dots). The bottom plot displays individual engagement metrics: Likes (blue crosses), Shares (red squares), Comments (brown triangles), and Emojis (purple diamonds). (b) The exogenous signal. The engagement trajectory of post p after the observation period under policy π_A , derived from Google Trends data, with a one-day exposure time (shaded area from day 7 to 8). The top plot shows observed engagement (solid blue line), predicted engagement without intervention (dashed blue line), and predicted engagement under π_A (dashed red line). The bottom plot displays normalized intensity λ_{obs} (dashed green line), policy π_A intensity (dashed red line), observed events (cyan dots), and policy actions (magenta dots). A vertical line at day 7 marks the intervention start. (c) The counterfactual signal. How the engagement trajectory of post p would have evolved if policy π_B had been applied during [0,7] with a three-day exposure time (shaded area from day 7 to 10). The top plot shows observed engagement (solid blue line), predicted engagement without intervention (dashed blue line), predicted engagement under π_A (dashed red line), and counterfactual engagement under π_B (solid orange line). The bottom plot displays normalized intensity λ_{obs} (dashed green line), counterfactual policy π_B intensity (dashed orange line), observed events (cyan dots), and policy actions (magenta dots). A vertical line at day 7 marks the intervention start.

cies. We achieve this by jointly modeling the bidirectional relationship between external signals and engagement outcomes.

3.1 Joint Treatment-Outcome Model

Inspired by the causal modeling framework of Hızlı et al. (2023), we propose a joint treatment-outcome model tailored for predicting social engagement in discrete-time social media data. While Hızlı et al. (2023) use marked point processes for treatment intensity and conditional Gaussian processes for continuous-time outcomes, we adapt this approach to discrete time using deep sequential models. This adaptation improves scalability and flexibility for large-scale, irregularly sampled social media datasets while preserving the bidirectional dependency between treatments (external signals) and engagement outcomes.

Treatment Intensity Modeling We model treatment intensity $\lambda_{\pi}^*(t)$ as the probability of a binary treatment event (e.g., a Google Trends spike) at each discrete time step t. The

intensity is computed via a square transformation of a latent function $g_{\pi}^{*}(t)$:

$$\lambda_{\pi}^{*}(t) = \left(\beta_{0} + g_{b}(t) + g_{a}^{*}(t) + g_{o}^{*}(t) + g_{g}^{*}(t)\right)^{2},$$

where β_0 represents a constant baseline intensity, $g_b(t)$ is a time-dependent baseline function, $g_a^*(t)$ models dependence on past treatments, $g_o^*(t)$ captures dependence on past engagement outcomes, and $g_g^*(t)$ incorporates Google Trends intensity.

For $g_g^*(t)$, we use discrete-time window sampling at 10-minute intervals ($\Delta_g = 10$ minutes):

$$g_g^*(t) = \sum_{k=0}^{w-1} \alpha_k \cdot g(t - k\Delta_g) \cdot \mathbf{1}_{[t-k\Delta_g, t-(k-1)\Delta_g)}(t),$$

Here, w is the number of historical windows considered, $g(t-k\Delta_g)$ is the Google Trends value at time $t-k\Delta_g$, α_k are learnable decay coefficients, and $\mathbf{1}_{[a,b)}(t)$ is an indicator function. $\lambda_{\pi}^*(t)$ is evaluated at discrete time steps, with treatments sampled as binary events based on this probability.

To align Google Trends with engagement observations, we implement a temporal alignment mechanism. For each observation time t_j , we collect signals within a lag window:

$$G(t_j) = \{g_k \mid t_j - \tau_{\text{lag}} \le t_k < t_j\}$$

where τ_{lag} is a hyperparameter determined through cross-validation. The resulting feature vector is $\mathbf{v}_g(t_i) = [g(t_i - \Delta_g), g(t_i - 2\Delta_g), \dots, g(t_i - w\Delta_g)]$.

3.2 Causal Assumptions

Our causal framework relies three key assumptions suitable for social media contexts:

Assumption 1 (Consistency). The potential engagement outcome Y[a] under a specific pattern of external signals a equals the observed engagement Y when those exact signals actually occur.

This assumes observed Google Trends-engagement relationships persist if patterns reoccur. In social media environments, this consistency is supported by the relative stability of engagement mechanisms—including recommendation algorithms, user interfaces, and notification systems—which function as reliable mediators between external signals and user behavior (Becker et al., 2017). Empirical evidence from Calderon et al. (2024) reinforces this view, as their Opinion Market Model (OMM) incorporating Google Trends signals consistently outperformed baselines in predictive accuracy by approximately 17% lower error rates. Similarly, Rizoiu et al. (2017) demonstrated superior popularity prediction results with their HIP model by assuming that viewcount is externally driven by sharing behavior (Muchnik et al., 2013) and explicitly accounting for that as an exogenous driver. They prove that HIP has the Linear Time-Invariant property which ensures that identical external stimuli produce consistent engagement responses regardless of when they occur. While acknowledging temporal constraints, we assert this assumption holds within reasonable timeframes where platform mechanics and user behavior patterns remain stable, prior to significant algorithm updates or shifts in engagement norms.

Assumption 2 (Fully-Mediated Policy Effect). *External signals (like Google Trends spikes) affect engagement outcomes through observable mechanisms rather than hidden pathways.*

This assumption states that external signals (like Google Trends spikes) affect engagement outcomes through observable mechanisms rather than hidden pathways (Bakshy et al., 2015). The causal process operates through a well-defined mediational sequence: exogenous search intensity signals \rightarrow heightened topical salience \rightarrow content exposure via platform mechanisms \rightarrow measurable engagement behaviors (e.g., likes, shares, comments). Calderon et al. (2024) empirically validated this pathway, showing that external signals affect both the attention market size and opinion distribution. Similarly, Bakshy et al. (2015) provide further evidence by showing how exposure mechanisms directly mediate the relationship between content availability and user engagement with diverse information. Rizoiu et al. (2017)

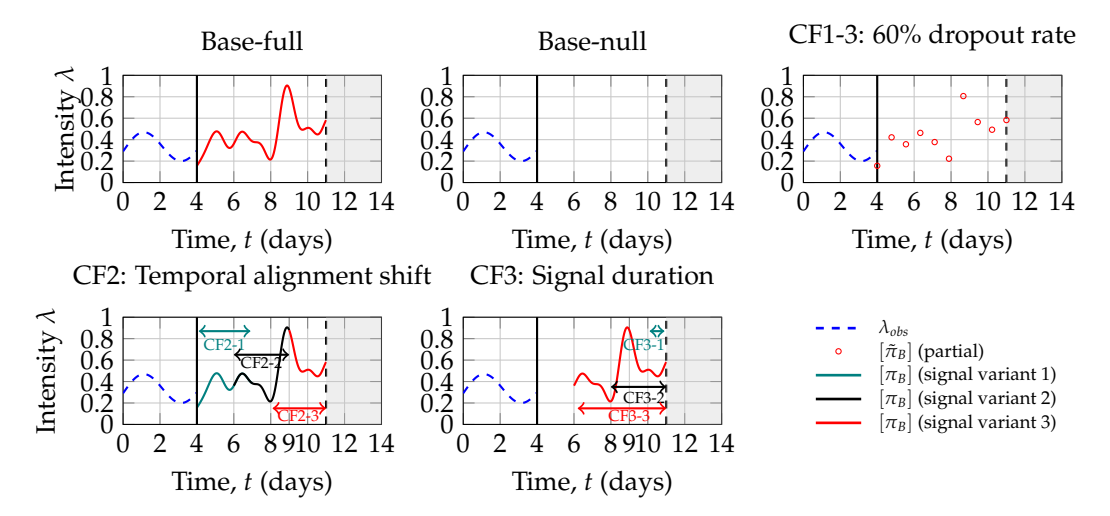


Figure 2: Engagement trajectory and counterfactual scenarios. Blue dashed lines represent observed social media engagement (λ_{obs}). Red lines indicate Google Trends signals ([π_B]). $\tilde{\pi}_B$ as the partial observed Google Trends signals. The vertical dashed line at day 9 marks the start of prediction period, with the gray shaded area showing the prediction region.

quantifies this relationship through their "popularity impulse response" function, measuring how external signals directly translate to viewership through measurable platform dynamics. Their simulated intervention experiments show that media coverage predictably shapes opinion market shares through these mechanisms. While alternative pathways might exist—such as algorithmic amplification or coordinated network activity—these appear to be minimal, as evidenced by both OMM's and HIP's superior predictive performance when directly modeling this attention-mediated relationship.

Assumption 3 (Temporal Precedence). Causes precede effects - current engagement can be influenced by past external signals but not by future ones.

This assumption aligns with the natural temporal ordering of social media interactions, where content engagement follows rather than precedes external attention signals. Rizoiu & Xie (2017a) provide strong empirical support through their temporally-sensitive Hawkes Intensity Process model, which demonstrates that popularity dynamics strictly follow the causal direction where external stimuli (like promotions) at time t can only influence engagement at times $\tau > t$, with a clear measurable *maturity time* quantifying this temporal lag. This maturity time metric captures the delay between external stimuli and the resulting engagement effects, providing a quantitative measure of the temporal precedence relationship. Their model's success in predicting YouTube viewcounts using this temporal framework validates the directional nature of the causal relationship. Similarly, Calderon et al. (2024) validate this in their Opinion Market Model, showing improved predictive performance when treating search trends as antecedent to engagement spikes. This temporal structure is further reinforced by platform mechanics, as content discovery algorithms typically respond to rising search interest by increasing content visibility, creating a causal chain that is unidirectional in time (Centola et al., 2018).

These assumptions, while not exhaustively verifiable, provide a reasonable foundation for causal inference in social media settings and allow us to identify treatment effects from observational data. Thus, building on the potential outcomes framework, we formulate our causal inference approach to estimate the effects of interventions on engagement trajectories.

3.3 Counterfactual Analysis

We introduce a counterfactual analysis framework that systematically manipulates exogenous signals along the temporal dimension to understand their causal impact on engagement dynamics, as shown in Figure 2. Formally, a counterfactual scenario $\mathcal C$ as a transformation of

the Google Trends signal $G = \{(t_k, g_k)\}_{k=1}^l$ through a temporal manipulation function Ψ_{θ} :

$$G_{\mathcal{C}} = \Psi_{\theta}(G) = \{(t_k + \delta_{\theta}(t_k, g_k), g_k \cdot \gamma_{\theta}(t_k, g_k))\}_{k=1}^l,$$

where δ_{θ} shifts the timing of signals and γ_{θ} adjusts signal intensity, enabling three counterfactual scenarios (CF): Dropout Rate (CF1) adjusts intensity (γ_{θ}) to explore exposure effects (0% \rightarrow 20% as CF1-1, 20% \rightarrow 40% as CF1-2, 40% \rightarrow 60% as CF1-3); Temporal Alignment Shifts (CF2) the onset timing (δ_{θ}) of a fixed-duration signal to test sensitivity to early exposure; Signal Duration Manipulation (CF3) modifies persistence to evaluate sustained attention effects (1-day as CF3-1, 3-day as CF3-2, 5-day as CF3-3). For each counterfactual scenario, we estimate the expected engagement outcomes under the transformed signal and calculate the causal effect as the difference between counterfactual and actual outcomes: $\Delta_{\mathcal{C}} = \mathbb{E}[Y|G_{\mathcal{C}}] - \mathbb{E}[Y|G]$.

3.4 Model Training and Optimization

We train our joint model using a combined loss function that explicitly optimizes both treatment intensity modeling and outcome prediction:

$$\mathcal{L}_{\text{joint}} = \underbrace{\text{MSE}(Y_{\text{true}}(t), Y_{\text{pred}}(t; \theta_{Y}))}_{\text{Outcome Loss}} + \alpha \underbrace{\text{BCE}(A_{\text{true}}(t), \lambda_{A}(t; \theta_{A}))}_{\text{Intensity Loss}}, \tag{1}$$

where α is a hyperparameter controlling the relative importance between accurate outcome prediction and accurate treatment intensity modeling. This joint optimization ensures that the model captures both the occurrence pattern of external signals (treatments) and their effects on engagement outcomes.

For the Mamba-based model, we additionally incorporate a temporal coherence loss, which ensures consistent state transitions across varying time intervals with $\mathcal{L}_{\text{temp}} = \frac{1}{|\mathcal{P}|} \sum_{p \in \mathcal{P}} \sum_{j=0}^{m-1} \|\mathbf{h}_{j+1} - \exp(\Delta t_j^+ \cdot \tilde{\mathbf{A}}_t) \mathbf{h}_j\|^2$. The temporal coherence loss regularizes the hidden state dynamics to follow the theoretical state transitions defined by the continuous-time state space model, where \mathbf{h}_j is the hidden state at time t_j , $\Delta t_j^+ = t_{j+1} - t_j$ is the forward time interval, and $\exp(\Delta t_j^+ \cdot \tilde{\mathbf{A}}_t)$ represents the state transition matrix over the interval Δt_j^+ . By minimizing this loss, we ensure that the model maintains consistent internal representations despite the irregular sampling intervals.

For the transformer-based model, we replace the temporal coherence loss with an attention consistency loss that encourages similar attention patterns for events with similar temporal relationships with $\mathcal{L}_{\text{att}} = \frac{1}{|\mathcal{P}|} \sum_{p \in \mathcal{P}} \sum_{i,j,k,l} w_{ijkl} \|\mathbf{A}_{ij} - \mathbf{A}_{kl}\|^2$. where \mathbf{A}_{ij} represents the attention weight from position i to position j, and w_{ijkl} is a similarity weight based on the temporal distance between positions.

4 Experiment and Results

This section introduces the datasets, models and baselines, and report our experimental findings on the optimal architecture choice for exogenously-driven engagement modeling.

4.1 Datasets

Social Media Engagement Data. The SocialSense dataset (Kong et al., 2022) is a misinformation dataset containing public Facebook posts collected between 2019 and 2021. It spans four domains: Australian Bushfires (78,030 posts), Climate Change (138,278 posts), Vaccination (178,894 posts), and COVID-19 (640,100 posts). These posts, labeled by domain experts, focus on misinformation and conspiratorial discussions. User engagements (likes, shares, comments, and emoji) were collected using the CrowdTangle API ².

²https://www.crowdtangle.com/before its termination in August 2024.

The DiN dataset (Tian et al., 2025) is a disinformation dataset comprising 746,653 posts from 41 accounts from 2019 to 2024. It is identified by social science experts as part of coordinated information operations. The posts are classified into 9 narratives based on the evaluation of the content.

External Signal Data from Google Trends. We collected Google Trends data to provide external signals aligned with both the temporal and thematic scope of the data sets. Keywords—selected via frequency analysis of post content and expert consultation—were theme-specific for SocialSense (e.g., "bushfire evacuation," "climate hoax") and narrative-specific for DiN (e.g., "election fraud," "deep state"). Using the Google Trends API 3 , the search information was retrieved via key phrases, normalized to 0–100, and retrieved at 10-minute intervals across the full temporal range of the social media datasets. These data were processed in an external signal timeline $G = (t_k, g_k)_{k=1}^l$, where g_k denotes the search interest at time t_k , and aligned with each post using a temporal lag window τ lag to model potential causal influences on engagement.

4.2 Models and Baselines

We evaluate eight architectural variants, four Transformer-based and four Mamba-based, each modified to incorporate external signals, with details in Appendix A.3.

Transformer-based Variants. We extend the Transformer (Vaswani et al., 2017) to model external signals via: +*Token* embeds tokenized signals with engagement data for joint self-attention; +*Attention* adds attention heads with custom masks for signal dependencies; +*Layer* processes signals via MLP, integrating with sequences through cross-attention; +*Adapter* inserts lightweight adapters (Houlsby et al., 2019) to model external signals.

Mamba-based Variants. We adapt Mamba (Gu & Dao, 2024), a selective state space model, to incorporate signals via: +*Token* embeds tokenized signals with engagement data for joint processing; +*Selection* conditions the selective scan on signal-engagement temporal relationships; +*Layer* processes signals via MLP, integrating outputs into Mamba's state; +*Adapter* adds adapters to condition state transitions on signal intensities.

We compare against three baselines: vanilla TimeSeries Transformer, Mamba and MBPP (Rizoiu et al., 2022), a marked point process that models engagement as a self-exciting process.

4.3 Results and Analysis

RQ1: Joint Modeling and Predictive Accuracy. Table 1 compares the performance of architectural variants under counterfactual perturbations (see scenarios of Section 3.3). *Mamba+Adapter* achieves the lowest RMSE (0.113) on baseline data, with selective state space models effectively capturing temporal engagement dependencies. As exposure levels increase, RMSE rises non-linearly, suggesting higher exposure renders engagement patterns more predictable through stronger signal regularization. Experiments reveal a 1-3 day optimal intervention window, with Mamba-based models handling temporally distant counterfactuals better than Transformer variants. Extended policy durations challenge all models, though *Transformer+Adapter* shows greater resilience to sustained signals. Appendix A.4 reveals disinformation (DiN dataset) poses greater challenges than misinformation, with higher base RMSE and larger increases at 60% exposure, suggesting inherently greater difficulty in predicting engagement with deliberately deceptive content.

RQ2: Architectural Differences in Temporal Causal Dependency Modeling. As shown in Table 2, *Mamba+Adapter* outperforms other architectures in capturing treatment dynamics, achieving the lowest BCE (0.35 at 60% exposure) with a 10.9% improvement over the best Transformer variant. An inverse relationship emerges between treatment intensity and modeling difficulty: BCE decreases from 0.488 to 0.350 as exposure rises from 20% to 60%. This suggests that high-intensity external signals may be more consistent with predictable patterns, offering potential for early detection of viral content trends. Temporal misalignment further amplifies architectural differences. For 5-day early interventions,

³https://serpapi.com/google-trends-api

Table 1: Root Mean Squared Error (RMSE) of engagement prediction over a 7-day horizon under counterfactual scenarios (see Section 3.3), averaged across two datasets. **Base**: Full exposure to external signal. **Scenario 1**: varying exposure levels (20%, 40%, 60%); **Scenario 2**: altered treatment timing (-5, -3, -1 days); **Scenario 3**: different treatment durations (1, 3, 5 days). Lower RMSE indicates better performance. '*' denotes no external signals.

Model	Base	Scena	rio 1: Ex	posure	Scena	ario 2: Tin	ning	Scena	rio 3: Du	ıration
		20%	40%	60%	-5 days	-3 days	-1 day	1-day	3-day	5-day
Transformer (Vaswani et al., 2017)	0.193*	_	_	_	_	_	_	_	_	_
Mamba (Gu & Dao, 2024)	0.189*	-	-	_	-	_	-	-	_	-
MBPP (Rizoiu et al., 2022)	0.193	0.326	0.295	0.281	0.225	0.225	0.226	0.329	0.315	0.284
Transformer + Token	0.128	0.214	0.220	0.225	0.210	0.203	0.197	0.238	0.245	0.250
Transformer + Attention	0.122	0.198	0.191	0.183	0.194	0.188	0.182	0.224	0.198	0.194
Transformer + Layer	0.125	0.202	0.194	0.187	0.198	0.192	0.186	0.228	0.202	0.198
Transformer + Adapter	0.115	0.190	0.183	0.176	0.186	0.180	0.175	0.216	0.190	0.186
Mamba + Token	0.129	0.205	0.197	0.190	0.201	0.195	0.189	0.245	0.225	0.218
Mamba + Selection	0.118	0.193	0.186	0.179	0.189	0.183	0.178	0.240	0.220	0.213
Mamba + Layer	0.120	0.195	0.188	0.180	0.191	0.185	0.179	0.242	0.222	0.215
Mamba + Adapter	0.113	0.185	0.178	0.171	0.181	0.176	0.170	0.236	0.218	0.210

Table 2: Binary Cross Entropy (BCE) evaluates treatment intensity prediction accuracy over a 7-day horizon across counterfactual scenarios, averaged across two datasets. Lower BCE reflects better modeling of temporal external signal patterns.

Model	Scena	rio 1: Ex	posure	Scen	ario 2: Tin	ning	Scenario 3: Treatment			
	20%	40%	60%	-5 days	-3 days	-1 day	1-day	3-day	5-day	
Transformer + Token	0.543	0.465	0.405	0.482	0.433	0.408	0.542	0.481	0.463	
Transformer + Attention	0.510	0.421	0.378	0.450	0.390	0.352	0.533	0.465	0.446	
Transformer + Layer	0.518	0.432	0.385	0.460	0.403	0.372	0.513	0.430	0.412	
Transformer + Adapter	0.495	0.402	0.355	0.428	0.372	0.339	0.545	0.482	0.464	
Mamba + Token	0.532	0.455	0.395	0.470	0.420	0.400	0.535	0.482	0.464	
Mamba + Selection	0.502	0.413	0.368	0.435	0.378	0.346	0.535	0.470	0.454	
Mamba + Layer	0.509	0.422	0.372	0.445	0.386	0.355	0.538	0.472	0.450	
Mamba + Adapter	0.488	0.398	0.350	0.420	0.365	0.335	0.525	0.465	0.440	

Mamba+Adapter demonstrates a 20.2% BCE advantage over Transformer+Token, showing the strength of state space models in managing temporally shifted causal processes.

RQ3: Counterfactual Robustness and Reliability. Table 3 reveals distinct patterns in causal relationships between external signals and engagement outcomes. The Mamba+Selection configuration estimates the highest ATE (0.635 ± 0.135 for CF1-3, $40\% \rightarrow 60\%$ exposure), surpassing alternatives by 16.1%. This benefits from its selective scan algorithm, which is good at isolating causally relevant temporal patterns. Exposure adjustment experiments indicate a super-linear relationship between signal intensity and engagement impact: ATE rises by 42.1% from $20\% \rightarrow 40\%$ (0.409) to $40\% \rightarrow 60\%$ (0.612) exposure levels, suggesting that concentrated bursts of attention yield disproportionately high engagement returns. Timing manipulations reveal a temporal window amplifying causal influence, with an average ATE ratio of 1.55 between 1-day and 5-day early interventions across models, suggesting that precise timing within narrower windows boosts engagement, informing optimal content scheduling and promotion strategies. Having identified the optimal architectural choice—Mamba+Adaptors, dubbed *causal-Mamba*—, we now turn to identifying causal influencers.

5 Case Study: Identifying Causal Influencers on Social Media

Causal effect influence. We use our causal-Mamba architecture to estimate the causal influence of a source – users, public page and groups. We use the source's posting behavior as the causal treatment (compared to no exogenous signal), and we estimate its impact on predicting engagement metrics (quotes, replies, retweets, favorites).

Table 3: Average Treatment Effect (ATE), computed via G-computation (Robins, 1986), quantifies causal impacts of interventions over a 7-day horizon with 95% bootstrap confidence intervals (\pm), normalized across four engagement metrics (likes, comments, emoji reactions, shares). Higher ATE indicates stronger effects.

Model	Ex	posure Adjustm	ent	I	Timing Adjustment		Du	Duration Adjustment				
	CF1-1 (0% → 20%)	CF1-2 (20% → 40%)	CF1-3 (40% → 60%)	CF2-1 (5-day early, day 0)	CF2-2 (3-day early, day 0)	CF2-3 (1-day early, day 0)	CF3-1 (1-day dur.)	CF3-2 (3-day dur.)	CF3-3 (5-day dur.)			
Transformer+Token	0.173 ± 0.109	0.334 ± 0.181	0.496 ± 0.102	0.146 ± 0.075	0.188 ± 0.060	0.221 ± 0.054	$ 0.162 \pm 0.046$	0.297 ± 0.086	0.425 ± 0.104			
Transformer+Attention	0.180 ± 0.050	0.349 ± 0.083	0.523 ± 0.111	0.158 ± 0.083	0.202 ± 0.067	0.245 ± 0.057	0.172 ± 0.052	0.312 ± 0.090	0.456 ± 0.111			
Transformer+Layer	0.161 ± 0.047	0.297 ± 0.075	0.443 ± 0.091	0.131 ± 0.067	0.170 ± 0.055	0.203 ± 0.048	$ 0.148 \pm 0.045$	0.269 ± 0.076	0.389 ± 0.094			
Transformer+Adapter	0.189 ± 0.052	0.364 ± 0.088	0.547 ± 0.117	0.166 ± 0.085	0.217 ± 0.071	0.257 ± 0.061	$ 0.184 \pm 0.056$	0.334 ± 0.097	0.479 ± 0.117			
Mamba+Token	0.197 ± 0.054	0.381 ± 0.091	0.574 ± 0.121	0.175 ± 0.090	0.230 ± 0.075	0.272 ± 0.065	0.192 ± 0.060	0.352 ± 0.102	0.503 ± 0.123			
Mamba+Selection	0.221 ± 0.060	$\textbf{0.425} \pm \textbf{0.101}$	0.635 ± 0.135	0.195 ± 0.099	$\textbf{0.256} \pm \textbf{0.084}$	$\textbf{0.301} \pm \textbf{0.074}$	$ $ 0.216 \pm 0.067	$\textbf{0.391} \pm \textbf{0.112}$	$\textbf{0.559} \pm \textbf{0.134}$			
Mamba+Layer	0.193 ± 0.052	0.371 ± 0.089	0.556 ± 0.118	0.170 ± 0.087	0.224 ± 0.073	0.264 ± 0.063	0.187 ± 0.058	0.340 ± 0.098	0.487 ± 0.119			
Mamba+Adapter	0.212 ± 0.058	0.409 ± 0.098	$\textbf{0.612} \pm \textbf{0.131}$	0.187 ± 0.096	0.246 ± 0.080	0.290 ± 0.069	0.208 ± 0.064	0.378 ± 0.109	0.538 ± 0.131			

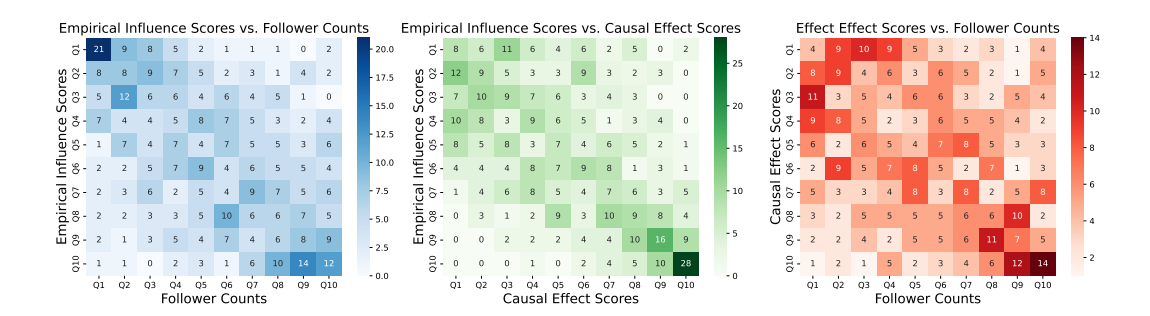


Figure 3: Decile Heatmaps (Spearman ρ correlation coefficient, Kendall's W rank agreement, Concordance Correlation Coefficient CCC): (**left**) Follower Counts vs. Empirical Influence ($\rho = 0.49$, W = 0.67, CCC = 0.00), (**centre**) Causal Effect vs. Empirical Influence (0.57, 0.70, 0.21), (**right**) Follower Counts vs. Causal Effect (0.32, 0.21, 0.01).

Baselines and datasets. There exists no universally accepted ground truth for measuring influence on social media. A popular proxy is the *number of followers*, as highly followed users are more likely to spread a content, possible leading to adoption (therefore, influence). The closest to a gold standard is the perceived *empirical influence* measure (Ram & Rizoiu, 2024), based on pairwise comparisons and an active learning-based ranking model. The empirical influence measure is based on human judgements, and has been shown to have desirable psychosocial properties. It is however prohibitive to scale; Ram & Rizoiu (2024) only computed it on 492 X/Twitter users, discussing anti-climate change topics.

Causal effect is a tighter approximation of influence. Fig. 4 shows pairs of Spearman correlation between the gold standard empirical influence and two approximations: the follower count and our proposed causal effect influence. Visibly, the causal effect is better estimation for empirical influence ($\rho=0.57$) than follower counts ($\rho=0.49$), particularly visible for the top 10% most influential users. Further analysis using Kendall's W confirms this stronger rank agreement between causal effect and empirical influence (W=0.70) compared to followers (W=0.67). The Concordance Correlation Coefficient reveals that while follower count fails entirely to capture the magnitude of influence (CCC=0.00), causal effect maintains some concordance (CCC=0.21). In particular, the two approximation measures themselves show minimal agreement ($\rho=0.32$, W=0.21, CCC=0.01), suggesting they capture fundamentally different aspects of influence. These results challenge the common assumption that account popularity (follower count) is a reliable approximation for true influence, demonstrating causal effect as a superior estimate both in ranking and scale.

Identify influential sources of misinformation. We analyzed the SocialSense dataset (Kong et al., 2022), focusing specifically on vaccination and climate change narratives. For each opinion, we calculated a weighted composite engagement score: $E(o) = \hat{e}_{likes}(o) + \hat{e}_{likes}(o)$

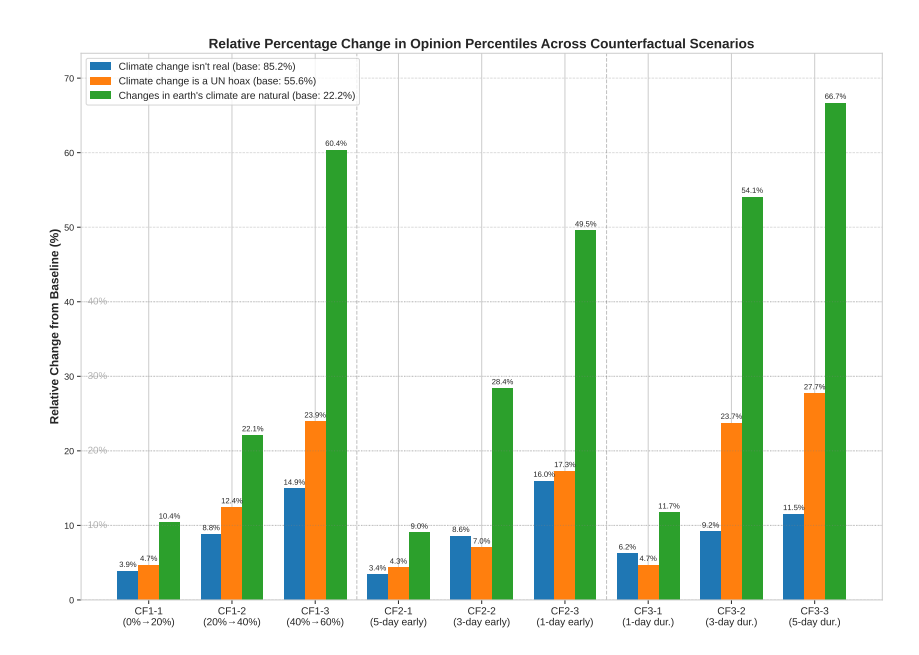


Figure 4: Relative percentage changes in engagement for three climate change misinformation narratives under counterfactual scenarios.

 $\hat{e}_{\mathrm{shares}}(o) + 3 \times \hat{e}_{\mathrm{comments}}(o) + \hat{e}_{\mathrm{emoji}}(o)$, then normalized these scores using percentile ranking: $P(o) = \frac{\mathrm{number\ of\ opinions\ with\ } E \leq E(o)}{\mathrm{total\ number\ of\ opinions\ }}$.

Our analysis extends viral potential theory Rizoiu & Xie (2017b) to misinformation contexts, confirming that content responsiveness to external promotion depends on baseline popularity and temporal dynamics across three climate change narratives: "Climate change isn't real" (85.2th percentile), "Climate change is a UN hoax" (55.6th percentile), and "Changes in earth's climate are natural" (22.2th percentile). Under progressive exposure manipulation (CF1), the lowest-baseline narrative exhibits super-linear amplification with a 6-fold scaling coefficient (10.4% \rightarrow 22.1% \rightarrow 60.4%), confirming that small external signals can trigger massive engagement increases. This behavior validates high-potential, low-baseline content theory (Rizoiu & Xie, 2017b), showing that emerging misinformation operates similarly to sleeping beauty content with high viral potential that have yet to achieve widespread attention but can rapidly amplify under external promotion. The intermediate narrative shows moderate scaling effects (4.7% \rightarrow 12.4% \rightarrow 23.9%), consistent with non-linear threshold dynamics in social influence, as evidenced by tipping point experiments (Centola et al., 2018). Temporal intervention analysis (CF2) reveals that initiating promotion one day earlier yields the highest amplification across all narrative types (16.0%, 17.3%, and 28.4%, respectively). This finding aligns with prior work on optimal promotion timing (Rizoiu & Xie, 2017b) and supports the broader framework of social acceleration (Rosa, 2013). Extended-duration experiments (CF3) show that a sustained 5-day exposure maximizes narrative amplification, with the emerging narrative reaching a 66.7% increase. This result corroborates the mere exposure effect (Zajonc, 1968), reinforcing the superiority of prolonged campaigns over short-term bursts.

Our causal model further identified influential public groups that amplified misinformation. For instance, @AustraliansforSafeTechnology increased the engagement score for "5G/smart tech is unsafe" narratives from 0.51 to 0.63 in February 2020, while @ClimateChangeBattleRoyale elevated "Climate change crisis isn't real" content from 0.11 to 0.23 in September 2019.

6 Conclusion

We investigate how external signals drive social media engagement, a key factor in misinformation and disinformation spread, using a straightforward joint treatment-outcome approach. By tweaking advanced models such as Transformers and Mamba, we improve the predictions of engagement under realistic policy treatments. Our approach faces *inherent causal challenges* including unobserved confounding from algorithmic amplification, selection bias in user engagement patterns, and treatment interference through network effects. Additional *limitations* include dependence on high-quality external signals that aren't always available, sensitivity to rapidly evolving platform algorithms, and assumptions of temporal stability in user behavior patterns. Despite these constraints, our case study proves our causal effect measure aligns closely with empirical influence, offering platforms and regulators a reliable metric to identify influential spreaders of misleading narratives.

Ethical Considerations and Dual-Use Concerns

This work uses publicly available social media data from platforms like X (formerly Twitter) and Facebook to analyze engagement patterns and misinformation dynamics. All data were collected in accordance with platform terms of service and API usage policies, and with approvals from our institution's Human Ethics Committee. Our analysis examines aggregate trends at the group level rather than targeting individuals. User identifiers were anonymized, and no personally identifiable information was collected or retained.

Our causal influence estimation framework has important ethical implications that extend beyond data privacy. While these tools enable beneficial applications like identifying sources of misinformation and improving platform governance, they could potentially be misused to optimize manipulation campaigns or target influential users for spreading harmful content. We acknowledge these dual-use concerns and propose safeguards, such as integrating with existing content moderation frameworks to prioritize intervention efforts.

We believe that understanding the causal mechanisms of influence is necessary for designing effective interventions against harmful content, and that responsible development practices—including limitations on individual-level influence measurements—can help mitigate potential misuse. Our research aims to contribute to the broader effort of creating healthier online information ecosystems while remaining mindful of these ethical challenges.

References

- Sinan Aral, Lev Muchnik, and Arun Sundararajan. Distinguishing influence-based contagion from homophily-driven diffusion in dynamic networks. *Proceedings of the National Academy of Sciences*, 106(51):21544–21549, 2009.
- Eytan Bakshy, Jake M Hofman, Winter A Mason, and Duncan J Watts. Everyone's an influencer: quantifying influence on twitter. In *Proceedings of the fourth ACM international conference on Web search and data mining*, pp. 65–74, 2011.
- Eytan Bakshy, Solomon Messing, and Lada A Adamic. Exposure to ideologically diverse news and opinion on facebook. *Science*, 348(6239):1130–1132, 2015.
- Jay J Van Bavel, Katherine Baicker, Paulo S Boggio, Valerio Capraro, Aleksandra Cichocka, Mina Cikara, Molly J Crockett, Alia J Crum, Karen M Douglas, James N Druckman, et al. Using social and behavioural science to support covid-19 pandemic response. *Nature human behaviour*, 4(5):460–471, 2020.
- Joshua Becker, Devon Brackbill, and Damon Centola. Network dynamics of social influence in the wisdom of crowds. *Proceedings of the national academy of sciences*, 114(26):E5070–E5076, 2017.
- Ioana Bica, Ahmed M Alaa, James Jordon, and Mihaela van der Schaar. Estimating counterfactual treatment outcomes over time through adversarially balanced repre-

- sentations. In *International Conference on Learning Representations*, 2020. URL https://openreview.net/forum?id=BJg866NFvB.
- Pio Calderon, Rohit Ram, and Marian-Andrei Rizoiu. Opinion market model: stemming far-right opinion spread using positive interventions. In *Proceedings of the international AAAI conference on web and social media*, volume 18, pp. 177–190, 2024.
- Qi Cao, Huawei Shen, Keting Cen, Wentao Ouyang, and Xueqi Cheng. Deephawkes: Bridging the gap between prediction and understanding of information cascades. In *Proceedings of the 2017 ACM on Conference on Information and Knowledge Management*, pp. 1149–1158, 2017.
- Damon Centola, Joshua Becker, Devon Brackbill, and Andrea Baronchelli. Experimental evidence for tipping points in social convention. *Science*, 360(6393):1116–1119, 2018.
- Meeyoung Cha, Hamed Haddadi, Fabricio Benevenuto, and Krishna Gummadi. Measuring user influence in twitter: The million follower fallacy. In *Proceedings of the international AAAI conference on web and social media*, volume 4, pp. 10–17, 2010.
- Justin Cheng, Lada Adamic, P Alex Dow, Jon Michael Kleinberg, and Jure Leskovec. Can cascades be predicted? In *Proceedings of the 23rd international conference on World wide web*, pp. 925–936, 2014.
- Tri Dao, Dan Fu, Stefano Ermon, Atri Rudra, and Christopher Ré. Flashattention: Fast and memory-efficient exact attention with io-awareness. *Advances in neural information processing systems*, 35:16344–16359, 2022.
- Keyan Ding, Ronggang Wang, and Shiqi Wang. Social media popularity prediction: A multiple feature fusion approach with deep neural networks. In *Proceedings of the 27th ACM International Conference on Multimedia*, pp. 2682–2686, 2019.
- Dean Eckles, René F Kizilcec, and Eytan Bakshy. Estimating peer effects in networks with peer encouragement designs. *Proceedings of the National Academy of Sciences*, 113(27): 7316–7322, 2016.
- Song Gao, Jinmeng Rao, Yuhao Kang, Yunlei Liang, Jake Kruse, Dorte Dopfer, Ajay K Sethi, Juan Francisco Mandujano Reyes, Brian S Yandell, and Jonathan A Patz. Association of mobile phone location data indications of travel and stay-at-home mandates with covid-19 infection rates in the us. *JAMA network open*, 3(9):e2020485–e2020485, 2020.
- Albert Gu and Tri Dao. Mamba: Linear-time sequence modeling with selective state spaces. In *First Conference on Language Modeling*, 2024. URL https://openreview.net/forum?id=tEYskw1VY2.
- Albert Gu, Tri Dao, Stefano Ermon, Atri Rudra, and Christopher Ré. Hippo: Recurrent memory with optimal polynomial projections. *Advances in neural information processing systems*, 33:1474–1487, 2020.
- Çağlar Hızlı, ST John, Anne Tuulikki Juuti, Tuure Tapani Saarinen, Kirsi Hannele Pietiläinen, and Pekka Marttinen. Causal modeling of policy interventions from treatment-outcome sequences. In *International Conference on Machine Learning*, pp. 13050–13084. PMLR, 2023.
- Neil Houlsby, Andrei Giurgiu, Stanislaw Jastrzebski, Bruna Morrone, Quentin De Laroussilhe, Andrea Gesmundo, Mona Attariyan, and Sylvain Gelly. Parameter-efficient transfer learning for nlp. In *International Conference on Machine Learning*, pp. 2790–2799. PMLR, 2019.
- Sarah J Jackson, Moya Bailey, and Brooke Foucault Welles. # HashtagActivism: Networks of race and gender justice. Mit Press, 2020.
- Quyu Kong, Emily Booth, Francesco Bailo, Amelia Johns, and Marian-Andrei Rizoiu. Slipping to the Extreme: A Mixed Method to Explain How Extreme Opinions Infiltrate Online Discussions. In *Proceedings of the International AAAI Conference on Web and Social Media*, volume 16, pp. 524–535, 2022.

- Quyu Kong, Pio Calderon, Rohit Ram, Olga Boichak, and Marian-Andrei Rizoiu. Intervalcensored transformer hawkes: Detecting information operations using the reaction of social systems. In *Proceedings of the ACM web conference* 2023, pp. 1813–1821, 2023.
- Haewoon Kwak, Changhyun Lee, Hosung Park, and Sue Moon. What is twitter, a social network or a news media? In *Proceedings of the 19th international conference on World wide web*, pp. 591–600, 2010.
- Cheng Li, Jiaqi Ma, Xiaoxiao Guo, and Qiaozhu Mei. Deepcas: An end-to-end predictor of information cascades. In *Proceedings of the 26th international conference on World Wide Web*, pp. 577–586, 2017.
- Bryan Lim. Forecasting treatment responses over time using recurrent marginal structural networks. *Advances in neural information processing systems*, 31, 2018.
- Judith J Lok. Statistical modeling of causal effects in continuous time. *The Annals of Statistics*, pp. 1464–1507, 2008.
- Xiaodong Lu, Shuo Ji, Le Yu, Leilei Sun, Bowen Du, and Tongyu Zhu. Continuous-time graph learning for cascade popularity prediction. In *Proceedings of the Thirty-Second International Joint Conference on Artificial Intelligence*, pp. 2224–2232, 2023.
- Lev Muchnik, Sinan Aral, and Sean J Taylor. Social influence bias: A randomized experiment. *Science*, 341(6146):647–651, 2013.
- Judea Pearl. Causality. Cambridge university press, 2009.
- Jonas Peters, Dominik Janzing, and Bernhard Schölkopf. *Elements of causal inference: foundations and learning algorithms*. The MIT Press, 2017.
- Jiezhong Qiu, Jian Tang, Hao Ma, Yuxiao Dong, Kuansan Wang, and Jie Tang. Deepinf: Social influence prediction with deep learning. In *Proceedings of the 24th ACM SIGKDD international conference on knowledge discovery & data mining*, pp. 2110–2119, 2018.
- Rohit Ram and Marian-Andrei Rizoiu. Empirically measuring online social influence. *EPJ Data Science*, 13(1):53, 2024.
- Marian-Andrei Rizoiu and Lexing Xie. Online popularity under promotion: Viral potential, forecasting, and the economics of time. In *International AAAI Conference on Web and Social Media (ICWSM '17)*, pp. 182–191, 2017a. URL https://aaai.org/ocs/index.php/ICWSM/ICWSM17/paper/view/15553https://arxiv.org/pdf/1703.01012.pdf.
- Marian-Andrei Rizoiu and Lexing Xie Xie. Online popularity under promotion: Viral potential, forecasting, and the economics of time. In *Proceedings of the International AAAI Conference on Web and Social Media*, volume 11, pp. 182–191, 2017b.
- Marian-Andrei Rizoiu, Lexing Xie, Scott Sanner, Manuel Cebrian, Honglin Yu, and Pascal Van Hentenryck. Expecting to be hip: Hawkes intensity processes for social media popularity. In *Proceedings of the 26th international conference on world wide web*, pp. 735–744, 2017.
- Marian-Andrei Rizoiu, Alexander Soen, Shidi Li, Pio Calderon, Leanne J Dong, Aditya Krishna Menon, and Lexing Xie. Interval-censored hawkes processes. *Journal of Machine Learning Research*, 23(338):1–84, 2022.
- James Robins. A new approach to causal inference in mortality studies with a sustained exposure period—application to control of the healthy worker survivor effect. *Mathematical modelling*, 7(9-12):1393–1512, 1986.
- James M Robins, Miguel Angel Hernan, and Babette Brumback. Marginal structural models and causal inference in epidemiology, 2000.
- Hartmut Rosa. Social acceleration: A new theory of modernity. Columbia University Press, 2013.

- Peter Schulam and Suchi Saria. Reliable decision support using counterfactual models. *Advances in neural information processing systems*, 30, 2017.
- Hossein Soleimani, Adarsh Subbaswamy, and Suchi Saria. Treatment-response models for counterfactual reasoning with continuous-time, continuous-valued interventions. In *33rd Conference on Uncertainty in Artificial Intelligence, UAI 2017*, 2017.
- Lin Tian, Emily Booth, Francesco Bailo, Julian Droogan, and Marian-Andrei Rizoiu. Before it's too late: A state space model for the early prediction of misinformation and disinformation engagement. *arXiv preprint arXiv:2502.04655*, 2025.
- Ashish Vaswani, Noam Shazeer, Niki Parmar, Jakob Uszkoreit, Llion Jones, Aidan N Gomez, Ł ukasz Kaiser, and Illia Polosukhin. Attention is all you need. In *Advances in Neural Information Processing Systems*, volume 30. Curran Associates, Inc., 2017. URL https://proceedings.neurips.cc/paper_files/paper/2017/file/3f5ee243547dee91fbd053c1c4a845aa-Paper.pdf.
- Jia Wang, Vincent W Zheng, Zemin Liu, and Kevin Chen-Chuan Chang. Topological recurrent neural network for diffusion prediction. In 2017 IEEE international conference on data mining (ICDM), pp. 475–484. IEEE, 2017a.
- Yongqing Wang, Huawei Shen, Shenghua Liu, Jinhua Gao, and Xueqi Cheng. Cascade dynamics modeling with attention-based recurrent neural network. In *IJCAI*, volume 17, pp. 2985–2991, 2017b.
- Duncan J Watts, David M Rothschild, and Markus Mobius. Measuring the news and its impact on democracy. *Proceedings of the National Academy of Sciences*, 118(15):e1912443118, 2021.
- Haixu Wu, Jiehui Xu, Jianmin Wang, and Mingsheng Long. Autoformer: Decomposition transformers with auto-correlation for long-term series forecasting. *Advances in neural information processing systems*, 34:22419–22430, 2021.
- Robert B Zajonc. Attitudinal effects of mere exposure. *Journal of personality and social psychology*, 9(2p2):1, 1968.
- Qingyuan Zhao, Murat A Erdogdu, Hera Y He, Anand Rajaraman, and Jure Leskovec. Seismic: A self-exciting point process model for predicting tweet popularity. In *Proceedings of the 21th ACM SIGKDD international conference on knowledge discovery and data mining*, pp. 1513–1522, 2015.
- Fan Zhou, Xovee Xu, Goce Trajcevski, and Kunpeng Zhang. A survey of information cascade analysis: Models, predictions, and recent advances. *ACM Computing Surveys* (*CSUR*), 54(2):1–36, 2021a.
- Haoyi Zhou, Shanghang Zhang, Jieqi Peng, Shuai Zhang, Jianxin Li, Hui Xiong, and Wancai Zhang. Informer: Beyond efficient transformer for long sequence time-series forecasting. In *Proceedings of the AAAI conference on artificial intelligence*, volume 35, pp. 11106–11115, 2021b.
- Simiao Zuo, Haoming Jiang, Zichong Li, Tuo Zhao, and Hongyuan Zha. Transformer hawkes process. In *International conference on machine learning*, pp. 11692–11702. PMLR, 2020.

A Appendix

A.1 Related Work

Our research lies at the intersection of social media engagement prediction, causal inference for sequential data, and advanced sequence modeling.

Social Media Engagement Prediction. Social media engagement prediction has evolved from early content and user-focused models (Cheng et al., 2014) to approaches incorporating network structures (Zhao et al., 2015) and temporal dynamics (Rizoiu et al., 2017). Recent deep learning advances include DeepCas (Li et al., 2017), which uses random walks and attention mechanisms for cascade prediction; SNPP (Ding et al., 2019), applying temporal point processes with recurrent architectures; and Topo-LSTM (Wang et al., 2017a), which models user interactions through topological structures. Graph-based approaches like DeepInf (Qiu et al., 2018) leverage network structures to predict user behaviors. Temporal dynamics have been addressed through several specialized frameworks. DeepHawkes (Cao et al., 2017) combines reinforcement learning with Hawkes processes, while HIP (Rizoiu et al., 2017) and MBPP (Rizoiu et al., 2022) model view count dynamics on YouTube. IC-TH (Kong et al., 2023) tackles interval-censored observations in retweet prediction, and OMM (Calderon et al., 2024) offers a cross-platform mathematical framework for predicting content spread.

While these approaches have cascade modeling, they typically rely on historical engagement patterns without considering external causal drivers. Our work explicitly models how external signals (like Google Trends) causally impact engagement dynamics.

Causal Inference for Sequential Data. Causal inference with sequential data builds on foundations like g-methods (Robins, 1986) and marginal structural models (Robins et al., 2000), which handle time-varying treatments and confounders. These approaches have been extended to continuous-time settings (Lok, 2008; Schulam & Saria, 2017). Neural approaches include Recurrent Marginal Structural Networks (Lim, 2018), which extend traditional causal models with recurrent architectures, and Counterfactual Recurrent Network (Bica et al., 2020), which uses adversarial learning to address time-varying confounding. For continuous-time treatments, researchers have developed personalized treatment response curves using Gaussian processes (Soleimani et al., 2017) and counterfactual frameworks for disease trajectory modeling (Schulam & Saria, 2017). Recently, Hızlı et al. (2023) introduced a joint treatment-outcome model combining marked point processes with Gaussian processes for healthcare policy interventions. These methods, while advanced, often lack the flexibility to capture social media's unique engagement dynamics and the complex temporal patterns of external influence.

State Space Models and Transformers for Sequence Modeling. Sequence modeling has recently been dominated by transformer architectures (Vaswani et al., 2017) and state space models. Time series adaptations include Informer (Zhou et al., 2021b), using ProbSparse self-attention, and Autoformer (Wu et al., 2021), leveraging auto-correlation for period-based dependencies. State Space Models (SSMs) have emerged as efficient alternatives for capturing long-range dependencies (Gu et al., 2020), processing extremely long sequences (Dao et al., 2022), and achieving competitive performance in language modeling (Gu & Dao, 2024). The Mamba architecture (Gu & Dao, 2024) introduced selective state space modeling, achieving state-of-the-art results with reduced computational requirements.

Despite these advances, few studies have applied modern SSMs to social media engagement prediction in causal contexts. Existing approaches typically rely on graph-based (Lu et al., 2023), RNN (Wang et al., 2017b), or transformer methods (Zuo et al., 2020) that assume uniform sampling or discrete snapshots, overlooking the fine-grained temporal patterns essential to engagement dynamics.

A.2 Training Details

Models are trained on 4x NVIDIA A100 GPUs with PyTorch, using the joint loss function from Section 3.4 ($\alpha=0.5$, $\beta=0.1$). Optimization uses AdamW with a learning rate of 10^{-4} , batch size of 64, and early stopping based on validation RMSE (patience = 10 epochs). Hyperparameters (e.g., $\tau_{lag}=24$ hours, w=6) are tuned via grid search.

A.3 Model Architecture Details

Our implementation uses a depth-L architecture with embedding dimension d and hidden dimension h. Here are the details for each integration mechanism:

Token Integration: For the token-based approach, external signals g_t at time t are embedded through a projection $\mathbf{E}_g \in \mathbb{R}^{|g| \times d}$:

$$\mathbf{e}_g^t = \text{Embedding}(g_t) = \mathbf{W}_g g_t + \mathbf{b}_g$$

These embedded tokens are then interleaved with engagement embeddings in the input sequence:

$$\mathbf{X} = [\mathbf{e}_1, \mathbf{e}_g^1, \mathbf{e}_2, \mathbf{e}_g^2, \dots, \mathbf{e}_n, \mathbf{e}_g^n]$$

Attention Integration: For attention-based integration, we modify the self-attention mechanism to include specialized heads focused on learning external signals. Given query \mathbf{Q} , key \mathbf{K} , and value \mathbf{V} matrices, we compute:

$$Attention(\mathbf{Q}, \mathbf{K}, \mathbf{V}) = \operatorname{softmax} \left(\frac{\mathbf{Q}\mathbf{K}^T}{\sqrt{d_k}} \odot \mathbf{M} \right) \mathbf{V}$$

where **M** is a masking matrix with elements $m_{ij} = \exp(-\beta |t_i - t_j|)$ that emphasizes temporally proximate signal-engagement pairs with decay parameter $\beta = 0.1$.

Layer Integration: Our layer-based approach processes external signals through a separate MLP layer:

$$\mathbf{h}_g^l = \mathrm{MLP}_g^l(\mathbf{h}_g^{l-1}) = \mathbf{W}_2^l \cdot \mathrm{GeLU}(\mathbf{W}_1^l \mathbf{h}_g^{l-1} + \mathbf{b}_1^l) + \mathbf{b}_2^l$$

which is merged with the main sequence representations through cross-attention at each layer l:

$$\mathbf{h}_{e}^{l} = \mathbf{h}_{e}^{l-1} + \text{CrossAttention}(\mathbf{h}_{e}^{l-1}, \mathbf{h}_{g}^{l}, \mathbf{h}_{g}^{l})$$

Adapter Integration: For adapter-based integration, we insert compact bottleneck modules after each self-attention and feed-forward layer:

$$\mathbf{h}_{out} = \mathbf{h}_{in} + \mathbf{W}_{up} \cdot \text{GeLU}(\mathbf{W}_{down} \cdot \mathbf{h}_{in} + \mathbf{b}_{down}) + \mathbf{b}_{up}$$

where $\mathbf{W}_{\text{down}} \in \mathbb{R}^{d \times r}$ and $\mathbf{W}_{\text{up}} \in \mathbb{R}^{r \times d}$ with bottleneck dimension r = d/8.

For the Mamba variants, we extend the selective state space model with signal-conditioned selection mechanisms. The state update equation* becomes:

$$\mathbf{h}_t = \mathbf{A}(\mathbf{g}_t)\mathbf{h}_{t-1} + \mathbf{B}(\mathbf{g}_t)\mathbf{x}_t$$

where the state transition matrix $\mathbf{A}(\mathbf{g}_t)$ and input projection $\mathbf{B}(\mathbf{g}_t)$ are conditioned on external signals \mathbf{g}_t through a low-rank adaptation:

$$\mathbf{A}(\mathbf{g}_t) = \mathbf{A}_0 + \Delta \mathbf{A} \cdot \sigma(\mathbf{W}_g \mathbf{g}_t)$$

The selective scan algorithm uses a similar signal-aware mechanism to compute selection weights, allowing the model to dynamically focus on relevant temporal dependencies based on external signal patterns.

A.4 Detailed Results Across Individual Datasets

This appendix presents detailed experimental results for the predictive performance of various model architectures across five distinct datasets: bushfire, covid, vaccination, climate change, and DiN. The tables provided here complement the aggregated results reported in Section 4.3, which represent the mean Root Mean Squared Error (RMSE) and Binary Cross Entropy (BCE) across these datasets. Here, we report individual dataset results to offer a granular view of model behavior under different counterfactual scenarios.

Model	Base	Scena	Scenario 1: Exposure			ario 2: Tir	ning	Scenario 3: Duration			
		20%	40%	60%	-5 days	-3 days	-1 day	1-day	3-day	5-day	
Transformer + Token	0.147	0.233	0.242	0.243	0.232	0.213	0.207	0.252	0.263	0.272	
Transformer + Attention	0.133	0.212	0.193	0.197	0.208	0.202	0.188	0.242	0.208	0.212	
Transformer + Layer	0.142	0.208	0.192	0.193	0.212	0.198	0.192	0.238	0.212	0.208	
Transformer + Adapter	0.123	0.192	0.173	0.182	0.188	0.182	0.173	0.222	0.188	0.192	
Mamba + Token	0.143	0.207	0.183	0.192	0.203	0.197	0.183	0.263	0.247	0.232	
Mamba + Selection	0.132	0.183	0.177	0.178	0.187	0.173	0.177	0.262	0.238	0.223	
Mamba + Layer	0.128	0.177	0.162	0.158	0.173	0.167	0.153	0.252	0.228	0.217	
Mamba + Aďapter	0.127	0.183	0.172	0.173	0.187	0.183	0.172	0.258	0.232	0.208	

Table 4: Root Mean Squared Error (RMSE) of predicted social media engagement metrics over a 7-day horizon under counterfactual scenarios for the DiN dataset.

Model	Scena	rio 1: Ex	posure	Scen	ario 2: Tin	ning	Scenario 3: Treatment			
	20%	40%	60%	-5 days	-3 days	-1 day	1-day	3-day	5-day	
Transformer + Token	0.592	0.502	0.438	0.527	0.458	0.437	0.583	0.522	0.488	
Transformer + Attention	0.543	0.442	0.403	0.487	0.403	0.377	0.582	0.498	0.487	
Transformer + Layer	0.563	0.457	0.417	0.493	0.432	0.393	0.562	0.463	0.437	
Transformer + Adapter	0.532	0.423	0.387	0.453	0.397	0.358	0.578	0.507	0.493	
Mamba + Token	0.577	0.488	0.437	0.503	0.457	0.433	0.572	0.513	0.497	
Mamba + Selection	0.547	0.442	0.393	0.457	0.403	0.367	0.568	0.507	0.483	
Mamba + Layer	0.552	0.443	0.397	0.463	0.407	0.368	0.572	0.497	0.483	
Mamba + Aďapter	0.533	0.427	0.378	0.452	0.388	0.362	0.558	0.493	0.477	

Table 5: Binary Cross Entropy (BCE) of treatment intensity predictions over a 7-day horizon for the DiN dataset across counterfactual scenarios.

Model	Base	Scena	rio 1: Ex	posure	Scen	ario 2: Tin	ning	Scenario 3: Duration		
		20%	40%	60%	-5 days	-3 days	-1 day	1-day	3-day	5-day
Transformer + Token	0.129	0.216	0.218	0.223	0.208	0.203	0.198	0.241	0.243	0.248
Transformer + Attention	0.123	0.198	0.193	0.183	0.193	0.188	0.183	0.223	0.198	0.193
Transformer + Layer	0.126	0.203	0.198	0.188	0.198	0.193	0.188	0.228	0.203	0.198
Transformer + Adapter	0.117	0.193	0.188	0.178	0.188	0.183	0.178	0.218	0.193	0.188
Mamba + Token	0.130	0.208	0.203	0.193	0.203	0.198	0.193	0.243	0.223	0.218
Mamba + Selection	0.119	0.198	0.193	0.183	0.193	0.188	0.183	0.238	0.218	0.213
Mamba + Layer	0.121	0.203	0.198	0.188	0.198	0.193	0.188	0.243	0.223	0.218
Mamba + Aďapter	0.114	0.188	0.183	0.173	0.183	0.178	0.173	0.233	0.218	0.213

Table 6: Root Mean Squared Error (RMSE) of predicted social media engagement metrics over a 7-day horizon under counterfactual scenarios for the climate change dataset.

Model	Scena	rio 1: Ex	posure	Scen	ario 2: Tin	ning	Scenario 3: Treatment			
	20%	40%	60%	-5 days	-3 days	-1 day	1-day	3-day	5-day	
Transformer + Token	0.538	0.463	0.403	0.478	0.433	0.408	0.538	0.478	0.463	
Transformer + Attention	0.508	0.423	0.378	0.448	0.393	0.353	0.528	0.463	0.443	
Transformer + Layer	0.513	0.433	0.383	0.458	0.403	0.373	0.508	0.428	0.413	
Transformer + Adapter	0.493	0.403	0.353	0.428	0.373	0.338	0.543	0.483	0.463	
Mamba + Token	0.528	0.453	0.393	0.468	0.418	0.398	0.533	0.478	0.463	
Mamba + Selection	0.498	0.413	0.368	0.438	0.378	0.348	0.533	0.468	0.453	
Mamba + Layer	0.503	0.423	0.373	0.448	0.388	0.358	0.538	0.473	0.448	
Mamba + Adapter	0.483	0.398	0.348	0.418	0.363	0.333	0.523	0.458	0.438	

Table 7: Binary Cross Entropy (BCE) of treatment intensity predictions over a 7-day horizon for the climate change dataset across counterfactual scenarios.

Model	Base	Scena	Scenario 1: Exposure			ario 2: Tir	ning	Scenario 3: Duration			
		20%	40%	60%	-5 days	-3 days	-1 day	1-day	3-day	5-day	
Transformer + Token	0.126	0.211	0.213	0.218	0.203	0.198	0.193	0.235	0.238	0.243	
Transformer + Attention	0.121	0.193	0.188	0.178	0.188	0.183	0.178	0.218	0.193	0.188	
Transformer + Layer	0.123	0.198	0.193	0.183	0.193	0.188	0.183	0.223	0.198	0.193	
Transformer + Adapter	0.114	0.188	0.183	0.173	0.183	0.178	0.173	0.213	0.188	0.183	
Mamba + Token	0.127	0.203	0.198	0.188	0.198	0.193	0.188	0.238	0.218	0.213	
Mamba + Selection	0.117	0.193	0.188	0.178	0.188	0.183	0.178	0.233	0.213	0.208	
Mamba + Layer	0.119	0.198	0.193	0.183	0.193	0.188	0.183	0.238	0.218	0.213	
Mamba + Adapter	0.112	0.183	0.178	0.168	0.178	0.173	0.168	0.228	0.213	0.208	

Table 8: Root Mean Squared Error (RMSE) of predicted social media engagement metrics over a 7-day horizon under counterfactual scenarios for the vaccination dataset.

Model	Scena	rio 1: Ex	posure	Scen	ario 2: Tin	ning	Scenario 3: Treatment			
	20%	40%	60%	-5 days	-3 days	-1 day	1-day	3-day	5-day	
Transformer + Token	0.533	0.458	0.398	0.473	0.428	0.403	0.533	0.473	0.458	
Transformer + Attention	0.503	0.418	0.373	0.443	0.388	0.348	0.523	0.458	0.438	
Transformer + Layer	0.508	0.428	0.378	0.453	0.398	0.368	0.503	0.423	0.408	
Transformer + Adapter	0.488	0.398	0.348	0.423	0.368	0.333	0.538	0.478	0.458	
Mamba + Token	0.523	0.448	0.388	0.463	0.413	0.393	0.528	0.473	0.458	
Mamba + Selection	0.493	0.408	0.363	0.433	0.373	0.343	0.528	0.463	0.448	
Mamba + Layer	0.498	0.418	0.368	0.443	0.383	0.353	0.533	0.468	0.443	
Mamba + Aďapter	0.478	0.393	0.343	0.413	0.358	0.328	0.518	0.453	0.433	

Table 9: Binary Cross Entropy (BCE) of treatment intensity predictions over a 7-day horizon for the vaccination dataset across counterfactual scenarios.

Base	Scena	rio 1: Ex	posure	Scena	ario 2: Tin	ning	Scenario 3: Duration			
	20%	40%	60%	-5 days	-3 days	-1 day	1-day	3-day	5-day	
0.123	0.208	0.213	0.218	0.203	0.198	0.193	0.235	0.238	0.243	
0.117	0.193	0.188	0.178	0.188	0.183	0.178	0.218	0.193	0.188	
0.119	0.198	0.193	0.183	0.193	0.188	0.183	0.223	0.198	0.193	
0.112	0.188	0.183	0.173	0.183	0.178	0.173	0.213	0.188	0.183	
0.124	0.203	0.198	0.188	0.198	0.193	0.188	0.238	0.218	0.213	
0.115	0.193	0.188	0.178	0.188	0.183	0.178	0.233	0.213	0.208	
0.117	0.198	0.193	0.183	0.193	0.188	0.183	0.238	0.218	0.213	
0.110	0.183	0.178	0.168	0.178	0.173	0.168	0.228	0.213	0.208	
	0.123 0.117 0.119 0.112 0.124 0.115 0.117	20% 0.123 0.208 0.117 0.193 0.119 0.198 0.112 0.188 0.124 0.203 0.115 0.193 0.117 0.198	20% 40% 0.123 0.208 0.213 0.117 0.193 0.188 0.119 0.198 0.193 0.112 0.188 0.183 0.124 0.203 0.198 0.115 0.193 0.188 0.117 0.198 0.193	20% 40% 60% 0.123 0.208 0.213 0.218 0.117 0.193 0.188 0.178 0.119 0.198 0.193 0.183 0.112 0.188 0.183 0.173 0.124 0.203 0.198 0.188 0.115 0.193 0.188 0.178 0.117 0.198 0.193 0.183	20% 40% 60% -5 days 0.123 0.208 0.213 0.218 0.203 0.117 0.193 0.188 0.178 0.188 0.119 0.198 0.193 0.183 0.193 0.112 0.188 0.183 0.173 0.183 0.124 0.203 0.198 0.188 0.198 0.115 0.193 0.188 0.178 0.188 0.117 0.198 0.193 0.183 0.193	20% 40% 60% -5 days -3 days 0.123 0.208 0.213 0.218 0.203 0.198 0.117 0.193 0.188 0.178 0.188 0.183 0.119 0.198 0.193 0.183 0.193 0.188 0.112 0.188 0.183 0.173 0.183 0.178 0.124 0.203 0.198 0.188 0.198 0.193 0.115 0.193 0.188 0.178 0.188 0.183 0.117 0.198 0.193 0.183 0.193 0.188	20% 40% 60% -5 days -3 days -1 day 0.123 0.208 0.213 0.218 0.203 0.198 0.193 0.117 0.193 0.188 0.178 0.188 0.183 0.178 0.119 0.198 0.193 0.183 0.193 0.188 0.183 0.112 0.188 0.183 0.173 0.183 0.178 0.173 0.124 0.203 0.198 0.188 0.198 0.193 0.188 0.115 0.193 0.188 0.178 0.183 0.178 0.117 0.198 0.193 0.183 0.193 0.188 0.117 0.198 0.193 0.183 0.193 0.188	20% 40% 60% -5 days -3 days -1 day 1-day 0.123 0.208 0.213 0.218 0.203 0.198 0.193 0.235 0.117 0.193 0.188 0.178 0.188 0.183 0.178 0.218 0.119 0.198 0.193 0.183 0.193 0.188 0.183 0.223 0.112 0.188 0.183 0.173 0.183 0.178 0.173 0.213 0.124 0.203 0.198 0.188 0.198 0.193 0.188 0.238 0.115 0.193 0.188 0.188 0.183 0.178 0.233 0.117 0.198 0.193 0.188 0.183 0.183 0.238 0.117 0.198 0.193 0.183 0.193 0.188 0.183 0.238	20% 40% 60% -5 days -3 days -1 day 1-day 3-day 0.123 0.208 0.213 0.218 0.203 0.198 0.193 0.235 0.238 0.117 0.193 0.188 0.178 0.183 0.178 0.218 0.193 0.119 0.198 0.193 0.183 0.193 0.188 0.183 0.218 0.193 0.112 0.188 0.183 0.173 0.183 0.178 0.178 0.173 0.213 0.188 0.124 0.203 0.198 0.188 0.198 0.193 0.188 0.238 0.218 0.115 0.193 0.188 0.178 0.188 0.183 0.178 0.233 0.218 0.117 0.193 0.188 0.188 0.183 0.178 0.233 0.213 0.117 0.193 0.188 0.188 0.183 0.178 0.233 0.213 0.117 0.198 0.193	

Table 10: Root Mean Squared Error (RMSE) of predicted social media engagement metrics over a 7-day horizon under counterfactual scenarios for the covid dataset.

Model	Scena	rio 1: Ex	posure	Scen	ario 2: Tin	ning	Scenar	Scenario 3: Treatment			
	20%	40%	60%	-5 days	-3 days	-1 day	1-day	3-day	5-day		
Transformer + Token	0.531	0.453	0.393	0.468	0.423	0.398	0.528	0.468	0.453		
Transformer + Attention	0.498	0.413	0.368	0.438	0.383	0.343	0.518	0.453	0.433		
Transformer + Layer	0.503	0.423	0.373	0.448	0.393	0.363	0.498	0.418	0.403		
Transformer + Adapter	0.483	0.393	0.343	0.418	0.363	0.333	0.533	0.473	0.453		
Mamba + Token	0.518	0.443	0.383	0.458	0.408	0.388	0.523	0.473	0.453		
Mamba + Selection	0.488	0.403	0.358	0.428	0.368	0.338	0.523	0.458	0.443		
Mamba + Layer	0.493	0.413	0.363	0.438	0.378	0.348	0.528	0.463	0.438		
Mamba + Aďapter	0.473	0.388	0.338	0.413	0.358	0.328	0.513	0.448	0.428		

Table 11: Binary Cross Entropy (BCE) of treatment intensity predictions over a 7-day horizon for the covid dataset across counterfactual scenarios.

Model	Base	Scena	rio 1: Ex	posure	Scen	ario 2: Tin	ning	Scenario 3: Duration		
		20%	40%	60%	-5 days	-3 days	-1 day	1-day	3-day	5-day
Transformer + Token	0.121	0.206	0.212	0.217	0.202	0.193	0.188	0.231	0.237	0.242
Transformer + Attention	0.116	0.192	0.187	0.173	0.186	0.178	0.172	0.216	0.191	0.183
Transformer + Layer	0.117	0.196	0.188	0.181	0.192	0.187	0.182	0.218	0.193	0.192
Transformer + Adapter	0.111	0.183	0.182	0.171	0.179	0.173	0.168	0.211	0.186	0.178
Mamba + Token	0.123	0.201	0.197	0.183	0.196	0.192	0.187	0.233	0.217	0.208
Mamba + Selection	0.113	0.188	0.186	0.176	0.183	0.181	0.173	0.232	0.211	0.207
Mamba + Layer	0.116	0.193	0.192	0.178	0.188	0.183	0.181	0.236	0.213	0.212
Mamba + Adapter	0.107	0.181	0.173	0.166	0.177	0.172	0.163	0.223	0.208	0.203

Table 12: Root Mean Squared Error (RMSE) of predicted social media engagement metrics over a 7-day horizon under counterfactual scenarios for the bushfire dataset.

Model	Scenario 1: Exposure			Scenario 2: Timing			Scenario 3: Treatment		
	20%	40%	60%	-5 days	-3 days	-1 day	1-day	3-day	5-day
Transformer + Token	0.522	0.447	0.383	0.462	0.413	0.392	0.518	0.461	0.443
Transformer + Attention	0.488	0.403	0.362	0.428	0.377	0.333	0.512	0.447	0.426
Transformer + Layer	0.497	0.417	0.363	0.442	0.383	0.357	0.492	0.408	0.397
Transformer + Adapter	0.473	0.387	0.338	0.412	0.353	0.327	0.523	0.467	0.443
Mamba + Token	0.512	0.433	0.377	0.452	0.402	0.378	0.517	0.463	0.447
Mamba + Selection	0.478	0.397	0.352	0.413	0.362	0.328	0.513	0.452	0.433
Mamba + Layer	0.483	0.407	0.353	0.427	0.372	0.342	0.517	0.453	0.432
Mamba + Aďapter	0.467	0.378	0.337	0.398	0.352	0.318	0.507	0.447	0.418

Table 13: Binary Cross Entropy (BCE) of treatment intensity predictions over a 7-day horizon for the bushfire dataset across counterfactual scenarios.